Characterization of Neuronal Tau Protein as a Target of Extracellular Signal-regulated Kinase

Haoling Qi, Sudhakaran Prabakaran, François-Xavier Cantrelle, Béatrice Chambraud, Jeremy Gunawardena, Guy Lippens, Isabelle Landrieu

THE JOURNAL OF BIOLOGICAL CHEMISTRY VOL. 291, NO. 14, pp. 7742–7753, April 1, 2016

Characterization of Neuronal Tau Protein as a Target of Extracellular Signal-regulated Kinase*

Received for publication, October 28, 2015, and in revised form, January 20, 2016 Published, JBC Papers in Press, February 8, 2016, DOI 10.1074/jbc.M115.700914

Haoling Qi[‡], Sudhakaran Prabakaran[§], François-Xavier Cantrelle[‡], Béatrice Chambraud[¶], Jeremy Gunawardena[§], Guy Lippens[‡], and Isabelle Landrieu[‡1]

From [‡]Lille University, CNRS UMR8576, F-59000 Lille, France, [§]Department of Systems Biology, Harvard Medical School, Boston, Massachusetts 02115, and [¶]INSERM UMR1195 Paris SUD University, Le Kremlin Bicêtre 94276, France

Tau neuronal protein has a central role in neurodegeneration and is implicated in Alzheimer disease development. Abnormal phosphorylation of Tau impairs its interaction with other proteins and is associated with its dysregulation in pathological conditions. Molecular mechanisms leading to hyperphosphorylation of Tau in pathological conditions are unknown. Here, we characterize phosphorylation of Tau by extracellular-regulated kinase (ERK2), a mitogen-activated kinase (MAPK) that responds to extracellular signals. Analysis of *in vitro* phosphorylated Tau by activated recombinant ERK2 with nuclear magnetic resonance spectroscopy (NMR) reveals phosphorylation of 15 Ser/Thr sites. *In vitro* phosphorylation of Tau using rat brain extract and subsequent NMR analysis identifies the same sites. Phosphorylation with rat brain extract is known to transform Tau into an Alzheimer disease-like state. Our results indicate that phosphorylation of Tau by ERK2 alone is sufficient to produce the same characteristics. We further investigate the mechanism of ERK2 phosphorylation of Tau. Kinases are known to recognize their protein substrates not only by their specificity for a targeted Ser or Thr phosphorylation site but also by binding to linear-peptide motifs called docking sites. We identify two main ERK2 docking sites in Tau sequence using NMR. Our results suggest that ERK2 dysregulation in Alzheimer disease could lead to abnormal phosphorylation of Tau resulting in the pathology of the disease.

Tau is an intrinsically disordered protein whose primary sequence is divided into several functional domains: an N-terminal region, a proline-rich domain (PRD),[2] a microtubule binding domain (MTBD) constituted of partially repeated sequences R1 to R4, and a C-terminal region (see Fig. 1*A*). Both PRD and MTBD are involved in microtubule stabilizing activity of Tau (1, 2).

Phosphorylation of Tau is an essential process to regulate its physiological function(s); however, abnormal phosphorylation of Tau has been linked to neuronal dysfunction (3–5). In Alzheimer disease (AD) Tau is hyperphosphorylated and aggregated (6). The longest Tau protein isoform (441 residues) has 80 threonine (Thr) or serine (Ser) residues. These residues are exposed as Tau is an intrinsically disordered protein subject to modification by numerous kinases (7). Mass spectrometry (MS) analyses have identified ~45 phosphorylated sites on Tau aggregates extracted from AD patients with a typical paired helical filament (PHF) morphology (8, 9) compared with 15–30 phosphorylation sites in soluble Tau extracted from mice (10) or normal human brain (11). Monoclonal antibodies such as AT8 (recognizing Ser(P)-202/Thr(P)-205; Ref. 12) or PHF1 (Ser(P)-396/Ser(P)-404; Ref. 13) are often used to detect abnormal phosphorylation of Tau (5). Proline-directed kinases with a (S/T)P phosphorylation consensus motif, such as cyclin-dependent kinase 5 (CDK5; Refs. 14 and 15) with its activator protein p25, glycogen synthase kinase (GSK3β; Ref. 16), stress-activated protein kinases (JNK; Ref. 17), and p38 (18) and extracellular-signal-regulated kinase (ERK1/2; Ref. 19), are considered as potential therapeutic targets to prevent Tau hyperphosphorylation (20). A clear understanding of the mechanism of abnormal phosphorylation of Tau leading to neuronal dysregulation is still lacking. Characterization of the kinases involved in the phosphorylation of Tau and the related specific patterns of phosphorylation are, therefore, of interest to develop new strategies to counteract the pathological processes.

ERK2 belongs to the mitogen-activated protein kinase (MAPKs) family and is activated by dual phosphorylation on a Thr-Xaa-Tyr sequence in its activation loop by MAP kinase kinases (MKK) (21–23). Human ERK2 is phosphorylated on Thr-183 and Tyr-185 by MEK kinase. MAP kinases have a classic kinase structure with an N-terminal lobe folded as a β sheet associated to a larger C-terminal domain constituted of α-helices (24). The activation loop is located at the hinge between these domains and shows a large conformational change upon phosphorylation (25). Mechanisms regulating specificity and efficiency of kinases are not fully understood but involve the binding of kinase docking grooves to binding motifs on their substrates, made up of a linear peptide (26, 27). Interaction regions distinct from the catalytic pocket were found to be involved in the recognition of both ERK1/2 upstream regulators and downstream substrates (28). The ERK docking site is

* This work was supported by TGE RMN THC (FR-3050, France) and FRABio (Lille University, CNRS, FR 3688) and also by a grant from the LabEx (Laboratory of Excellence), DISTALZ (Development of Innovative Strategies for a Transdisciplinary approach to Alzheimer's disease), and in part by the French government funding agency Agence Nationale de la Recherche TAF. This work was supported by National Institutes of Health Grant R01 GM081578 (to S. P. and J. G.). The authors declare that they have no conflicts of interest with the contents of this article. The content is solely the responsibility of the authors and does not necessarily represent the official views of the National Institutes of Health.

[1] To whom correspondence should be addressed: RMN, IRI Building (CNRS) Parc Scientifique de la Haute Borne 50, avenue de Halley, 59650 Villeneuve d'Ascq, France. Tel.: 33362531702; E-mail: isabelle.landrieu@univ-lille1.fr.

[2] The abbreviations used are: PRD, proline rich domain; AD, Alzheimer disease; MTBD, microtubule binding domain; PHF, paired helical filament; HSQC, heteronuclear single quantum correlation.

targeted by proteins that contain a linear motif called the D-recruitment site (DRS or D-site), defined by a loose consensus of ~10 amino acid residues $\Psi_{1-3}\,X_{3-7}\,\Phi X\,\Phi$ (Ψ, Φ, and X refer to positively charged, hydrophobic, or any intervening residues, respectively, and subscripts refer to the number of residues (30)). Interactions of the conserved D-recruitment site motifs with the MAP kinase docking site has been characterized at the atomic level in complexes of ERK2 with peptide fragments from several protein partners (30–33). In addition, another docking motif was identified, called F-recruitment site (FRS or F-site) that recognizes a Phe-Xaa-Phe motif (34).

ERK1/2 activation in AD brain is well documented (35–37). Results from previous studies indicate that ERK1/2 is able to transform Tau into an AD-like state, but this is mainly documented by the detection of the epitope recognized by the AT8 antibody (19). To better define the phosphorylation sites involved in the transformation of Tau as present in AD (19), we used NMR spectroscopy. We observed that 14 out of the 17 S/T sites, which are followed by proline ((S/T)P sites) and likely to be recognized by proline-directed ERK1/2, are phosphorylated by activated recombinant ERK2 *in vitro*. Another well known *in vitro* model of Tau hyperphosphorylation is obtained by incubation of Tau with rat brain extracts along with phosphatase inhibitor okadaic acid (38). We compared the phosphorylation pattern of Tau obtained using rat brain extract with that obtained using the *in vitro* activated recombinant ERK2. A similar pattern of Tau phosphorylation was indeed observed, which strongly suggests that ERK2 is sufficient for hyperphosphorylation of Tau. We then studied the Tau-ERK2 interaction. We mapped the interaction sites of ERK2 along the Tau sequence and identified two docking sites in the MTBD, which is distal to the PRD containing most of the ERK phosphorylated sites of Tau. We, therefore, conclude that Tau and ERK2 form a dynamic complex. Our study indicates that Tau could be the first example of an ERK2 substrate with multiple docking sites. These conclusions expand our view on the potential role of ERK2 in the neurodegeneration pathway in AD involving Tau and shed light on the molecular mechanisms leading to pathological Tau formation.

Experimental Procedures

Molecular Cloning—cDNA encoding peptides Tau-(220–240) and Tau-(271–294) were amplified from Tau full-length cDNA by PCR. The cDNA were cloned by a ligation-independent protocol into vector pETNKI-HisSUMO3-LIC (39).

Preparation of Recombinant Proteins—The longest isoform of Tau (441 amino acid residues) and the Tau fragments Tau-(165–245) and Tau-(244–372) (K18) were expressed and purified as recombinant proteins from *Escherichia coli* Bl21(DE3) (New England BioLabs) using pET15b plasmid (Invitrogen) under the control of T7lac promoter. Tau fragments Tau-(220–240) and Tau-(271–294) were expressed as N-terminal fusion with the SUMO protein presenting a N-terminal His tag from a modified pET vector (39).

Bacteria were grown in LB medium at 37 °C and recombinant protein production induced with 0.4 mM isopropyl-1-thio-β-D-galactopyranoside. Isotope labeling was performed using a modified M9 medium containing in addition to the M9 salts, minimum Eagle's medium vitamin mix 1× (Sigma), 1 g of $[^{15}N]NH_4Cl$, 4 g of glucose or 2 g of [^{13}C]glucose and 200 mg of complete medium powder (Celtone Complete Medium, Cambridge Isotope Laboratories) per liter of bacterial culture. Briefly, Tau protein, Tau-(165–245) and Tau-(244–372) fragments were purified by first heating the bacterial extract 15 min at 75 °C. Purification consisted of cation exchange chromatography with a sodium phosphate buffer at pH 6.5 (Hitrap SP-Sepharose FF, 5 ml; GE Healthcare) for Tau and Tau-(165–245) and nickel-chelating chromatography for Tau-(244–372) (Hitrap nickel-Sepharose FF, 5 ml; GE Healthcare). Full-length Tau protein and Tau fragments were then buffer-exchanged against ammonium bicarbonate (Hiload 16/60 desalting column, GE Healthcare) for lyophilization. His-SUMO Tau-(220–240) and His-SUMO Tau-(271–294) were purified by affinity chromatography on nickel-nitrilotriacetic acid resin following the manufacturer's protocols. The fusion proteins were buffer-exchanged using a PD-10 column (G25 resin, cutoff of 7 kDa; GE Healthcare) against NMR buffer.

Recombinant His_6-tagged p42 MAP kinase (ERK2) from *Xenopus laevis* was prepared by growing bacteria transformed with a ERK recombinant T7 expression plasmid in LB medium until induction by 1 mM isopropyl 1-thio-β-D-galactopyranoside of the protein production for a period of 4 h at 37 °C. His-ERK2 was purified using nickel-nitrilotriacetic acid-based affinity chromatography following the manufacturer's protocols. After analysis on SDS-PAGE, the pooled fractions were buffer-exchanged using a PD-10 column (GE Healthcare) against conservation buffer 50 mM Tris-HCl, 150 mM NaCl, 0.1 mM EGTA, 50% glycerol, pH 7.5, and kept frozen at −80 °C. His_6-tagged D321N/D324N ERK2 was prepared in the same manner. Activated-ERK2 was prepared as previously described by *in vitro* incubation with activated MEK (40).

To label Tau with CF3 attached on its native Cys residues (Cys-291 and Cys-322), 100 μM [^{15}N]Tau or [^{15}N]Tau-(244–372) in 50 mM ammonium bicarbonate were first thoroughly reduced by incubation for 2 h at 22 °C with 1 mM Tris (hydroxymethyl) phosphine reducing agent. The protein samples were next incubated with 2 mM 2-iodo-*N*-trifluoroethyl acetamide (EnamineStore) in dimethyl sulfoxide at 22 °C for 3 h. The excess of 2-iodo-*N*-trifluoroethyl acetamide was removed by desalting. The CF_3-[^{15}N]Tau samples were lyophilized.

In Vitro Phosphorylation of Tau Protein—^{15}N-Labeled recombinant Tau was used as substrate to assay the activity of activated ERK2. 100 μM [^{15}N]Tau or [^{15}N]Tau-(165–245) was incubated with 1 μM ERK2 enzyme at 37 °C for 3 h in 200 μl of phosphorylation buffer 50 mM Hepes, pH 8.0, 50 mM NaCl, 12.5 mM $MgCl_2$, 2.5 mM ATP, 2 mM DTT, 1 mM EDTA, 2 mM EGTA, and protease inhibitor mixture (Roche Applied Science, Complete Inhibitors without EDTA). To identify the phosphorylation sites by NMR spectroscopy ^{13}C,^{15}N-double-labeled Tau was incubated in the same conditions overnight with the activated recombinant ERK2. Enzymatic incubation was terminated by heating the reaction mixture for 15 min at 75 °C followed by centrifugation. The phosphorylation mixture was buffer-exchanged using desalting centrifugal devices (0.5-ml-bed G25 resin, cutoff of 7 kDa, Thermo Scientific Zeba Desalting Columns) against NMR buffer (50 mM deuterated Tris, pH

6.65, 25 mM NaCl, 2.5 mM EDTA, 1 mM DTT and 10% D_2O). Phosphorylation of the Tau-(165–245) by ERK2 followed the same protocol. For the time course of phosphorylation, 100 μM [^{15}N]Tau was incubated for 15, 30, 60, 120, and 180 min with 1 μM activated-ERK2 as described above. The reaction was stopped by heating the sample at 75 °C for 15 min. The experiment was repeated three times.

The rat brain extract was prepared by homogenizing a brain (~2 g) in 5 ml of homogenizing buffer (10 mM Tris·Cl, pH 7.4, 5 mM EGTA, 2 mM DTT, 1 μM okadaic acid (Sigma) supplemented with 20 μg/ml leupeptin and 40 mM Pefabloc (38). Ultracentrifugation was next performed at 100,000 × *g* for 1 h at 4 °C. The supernatant was directly used for its kinase activity. Total protein concentration was estimated to be 7 mg/ml by the Bradford colorimetric assay. The [^{15}N]Tau protein (1–1.5 mg) was dissolved at 10 μM in 2.5 ml of phosphorylation buffer (2 mM ATP, 40 mM Hepes·KOH, pH 7.3, 2 mM $MgCl_2$, 5 mM EGTA, 2 mM DTT complemented with a protease inhibitor mixture (Roche Applied Science) and 1 μM okadaic acid (Sigma). The phosphorylation reaction was performed at 37 °C for 24 h with 500 μl of brain extract. Enzymatic incubation was terminated by heating the reaction mixture for 15 min at 75 °C followed by centrifugation. Phosphorylation mixture was buffer-exchanged against 50 mM ammonium bicarbonate before lyophilization. Phosphorylation of the Tau-(165–245) by rat brain extract kinase activity followed the same protocol. The samples were prepared by solubilizing the lyophilized powder into NMR buffer. Each set of experiment was independently repeated two or three times.

NMR Spectroscopy—Analysis of the phospho-Tau samples by NMR spectroscopy was performed at 293 K or 298 K on Bruker 600-MHz and 900-MHz spectrometers equipped with a triple resonance cryogenic probehead (Bruker, Karlsruhe, Germany). Trimethylsilyl propionate was used as the reference (0 ppm). 100 μM [^{15}N]Tau in a volume of 200 μl in 3-mm tubes was sufficient to obtain the two-dimensional ^{1}H,^{15}N heteronuclear single quantum correlation (HSQC) spectra with 32 scans. HSQC two-dimensional experiments to map the interaction between Tau protein and recombinant ERK2 were recorded at 293 K on a 900-MHz spectrometer with 64 scans per increment as a complex matrix of 2048 × 416 complex points for 14 × 25 ppm spectral widths in the proton and nitrogen dimensions, respectively. Three-dimensional HNCACB spectra were recorded for ^{13}C,^{15}N-phospho-Tau obtained both with rat brain extract and recombinant ERK2 with a standard Bruker pulse sequence. A three-dimensional HNcaNNH spectrum (41) was additionally used in the assignment. Three-dimensional HNCACB experiments were acquired to confirm the assignment of the Tau residues in ^{13}C,^{15}N-His-SUMO Tau-(220–240) and ^{13}C,^{15}N-His-SUMO Tau-(271–294). For Fluor NMR experiments, the lyophilized CF_3-[^{15}N]Tau and CF_3-[^{15}N]Tau-(244–372) were suspended in phosphate NMR buffer consisting of phosphate buffered saline, pH 7.4, 2.5 mM EDTA, and 2 mM DTT. 50 μM CF_3-Tau or CF_3-Tau-(244–372) in 200 μl of phosphate NMR buffer were titrated with increasing concentration of His-ERK2 (25, 50, 100, 125, 162, and 220 μM). The one-dimensional ^{19}F spectra were recorded at 293 K with 1024 scans on a Bruker 600MHz Avance NMR spectrometer equipped with a 5-mm CPQCI ^{19}F/^{1}H-^{13}C/^{15}N cryogenic probehead (Bruker). The chemical shifts in one-dimensional ^{19}F spectra were referenced by using the fluor resonance of external Trifluoroacetic acid at −76.55 ppm.

NMR Data Processing—Spectra were processed with Bruker TopSpin 3.1 software. Data analysis, peak picking, and calculation of peak volumes were done with Sparky 3.114 software (T. D. Goddard and D. G. Kneller, SPARKY 3, University of California, San Francisco). Assignment of resonances of Thr(P)- and Ser(P)-phosphorylated residues is based on the typical Cα and Cβ chemical shifts of these residues (42). Ser(P) and Thr(P) resonances were assigned to a specific residues in phospho-Tau primary sequence using as additional information the ^{15}N Cα and Cβ chemical shifts of their N-terminal residues (43–45) (Table 1). Resonance integration was performed in two-dimensional spectra by summing all the intensities over a box enclosing the peak of interest. To account for variations between spectra, integration volumes were normalized to the integration value of the resonance of Glu-62 residue, which is isolated in the spectrum and not influence by phosphorylation(s). To estimate the level of phosphorylation at each site, we first estimated the level of phosphorylation on Thr-153 residue using the resonances of Ala-152. Ala-152 has two distinct resonances in the two-dimensional ^{1}H,^{15}N spectrum depending on the phosphorylation status of Thr-153 residue. The ratio of the integration volumes of these Ala-152 resonances gives an estimation of the phosphorylation degree of Thr-153. We next used this value to correlate integration volumes of resonances with phosphorylation level of the corresponding phospho-residue.

In Vitro Aggregation Assay—Tau aggregation assays were performed at 0.25 mg/ml (5 μM) Tau (incubated overnight with activated recombinant ERK2 kinase in absence of ATP) or phosphorylated Tau in MES buffer consisting of 100 mM MES, pH 6.9, 2 mM EGTA, 1 mM $MgCl_2$, and 0.3 mM freshly prepared DTT. The samples were incubated at 35 °C with shaking at 300 rpm. After 2 h of incubation, the insoluble fraction was collected by centrifugation at 16,500 × *g*, and the pellet was suspended in 50 μl.

10-μl samples were applied on 400-mesh hexagonal Formvar-coated copper grids for 45 s. The sample-loaded grids were washed twice by ion-free water and drained. The grids were next negatively stained with 2% urinyl acetate solution for 60 s. The observation was performed by transmission electron microscopy (Hitachi H7500 at 80 kV and JEOL JEM-2100 at 200 kV.

Interaction of ERK2 with Tau, Tau Fragments, and Tau Peptides—ERK2 buffer exchange after storage was done using desalting centrifugal devices (1.5-ml-bed of G25 resin, cutoff of 7 kDa; Thermo Scientific Zeba Desalting Columns). ERK2 protein in Tris NMR buffer was then concentrated to a volume of 200 μl using a centrifugal concentrator (0.5 ml, 30 K membrane, Amicon Ultra) up to 250 μM. The concentrated enzyme solution was directly used to suspend lyophilized [^{15}N]Tau, [^{15}N]Tau-(244–372) (K18) and [^{15}N]Tau-(165–245) to a final concentration of 50–80 μM labeled samples. For the interaction with Tau peptides, ^{15}N-His-Sumo Tau-(220–240) peptide or ^{15}N-His-SUMO Tau-(271–294) peptide were directly mixed

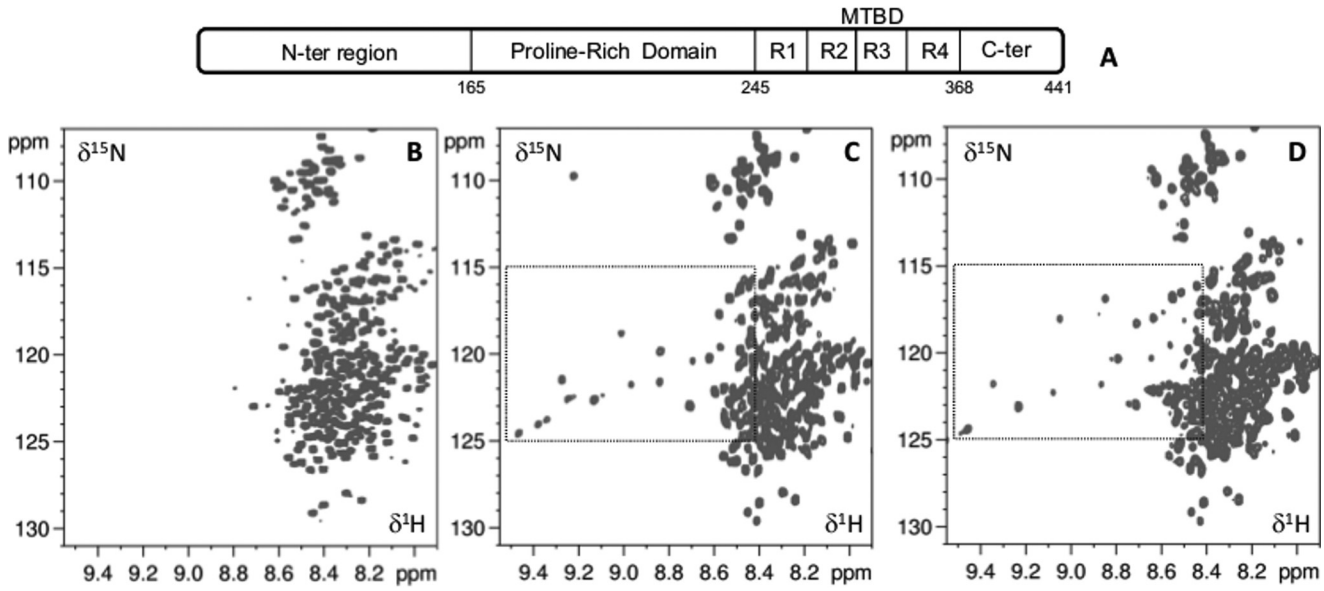

FIGURE 1. **Phosphorylation of Tau.** *A*, scheme of the domain organization of Tau protein. Limits of the domains are indicated by the amino acid number in the sequence. *B–D*, $^{1}H,^{15}N$ HSQC two-dimensional spectra of Tau (*B*), Tau phosphorylated by MEK-activated recombinant ERK2 (*C*), and Tau phosphorylated by rat brain extract kinase activity (*D*). The region of the spectrum containing resonances corresponding to phosphorylated S/T residues is *boxed* in *C* and *D* spectra. Detailed annotation of the resonances corresponding to phosphorylated residues is provided in Fig. 2*B*.

with ERK2 in the NMR buffer to a final concentration of 50 μM concentrations of labeled peptides. The ERK2 samples were prepared freshly before the NMR experiments due to the tendency of the ERK2 protein to precipitate in the NMR buffer conditions.

Results

Identification of Tau Amino Acids Phosphorylated in Vitro by ERK2—We used NMR spectroscopy to identify phosphorylation sites of Tau modified *in vitro* by activated ERK2. On incubation with MEK-activated recombinant ERK2 (double-phosphorylated on Thr-183/Tyr-185), several additional resonances were observed in the $^{1}H,^{15}N$ two-dimensional spectrum for the resulting phospho-Tau compared with the spectrum of the unphosphorylated Tau (compare Fig. 1, *B* and *C*). These resonances are typical for the HN amide resonances of Ser(P) and Thr(P) residues (42, 44), indicating that Tau is indeed phosphorylated at many sites by ERK2. Phosphorylation sites were identified using three-dimensional triple resonance NMR spectroscopy on a $^{13}C,^{15}N$-labeled Tau sample phosphorylated *in vitro* by activated ERK2. Of the 17 (S/T)P sites, 14 sites along the Tau sequence were found to be phosphorylated by ERK2 (Fig. 2, *A* and *B*; Table 1). ERK2 phosphorylated Thr-50, Thr-153, Thr-175, Thr-181, Thr-205, Thr-231, Ser-235, Ser-404, and Ser-422 with a stoichiometry of >50%; estimation was based on peak integration (45) (Fig. 2*B*, Table 1). In addition, a minor phosphorylation was observed for Ser-191, which is not a Pro-directed site (Fig. 2, Table 1). Phosphorylation by ERK2 of a Tau-(165–245) fragment encompassing the PRD of Tau allowed confirmation of the identification of the phosphorylation sites located in this domain (Fig. 2*C*). A comparison with previous assignments of the NMR amide cross-peaks corresponding to Tau proline-directed phosphorylation sites, generated by cyclin-dependent kinase 2/CycA3 or glycogen synthase kinase 3 (GSK3) (46, 47), further confirmed identification of the ERK2 phosphorylation sites located in the PRD and C-terminal region. Kinetic experiments were next performed to define the order of the multiple phosphorylations of Tau by recombinant ERK2. SDS-PAGE analysis of Tau during a time-course of phosphorylation by activated ERK2 showed a gradual decreased mobility associated with a global increase of Tau phosphorylation level (Fig. 3*A*). A series of two-dimensional spectra was then acquired corresponding to various incubation times to get insight at site-specific time-dependent modification of Tau by ERK2. The level of modification at each identified phosphorylation site was estimated by the integral of the corresponding resonance. The fastest observed phosphorylation was found for Ser-235, Ser-404, and Ser-422 followed by Thr-50, Thr-181, and Thr-205 (Fig. 3, *B–D*). The time-dependent phosphorylation increase for these residues can be fitted with an exponential function, with rate constants ranging from 10 to 85 min. Slower modification was observed for residues Ser-46, Thr-69, Thr-153, Thr-175, Ser-191, Ser-199, Thr-231, and Ser-396, which showed a linear trend of phosphorylation increase during the 3-h time course of Tau incubation with activated-ERK2.

Comparison of ERK2-phosphorylated Tau with a Hyperphosphorylation Model of Tau—Phosphorylation of S/T residues corresponding to 12–15 sites has similarly been reported after incubation of Tau with rat brain extract (12, 38, 48). The site-specific, precise pattern of the hyperphosphorylation of Tau by rat brain extract was, however, never investigated. We, therefore, used NMR spectroscopy to establish the map of Tau amino acid residues phosphorylated by kinases in rat brain extract and compared with those phosphorylated by ERK2. Rat brain extracts were used to *in vitro* phosphorylate recombinant ^{15}N-labeled Tau. The corresponding $^{1}H,^{15}N$ two-dimensional spectrum of the phosphorylated Tau showed additional resonances in the region for Thr(P) and Ser(P) residues compared with the spectrum of the unphosphorylated Tau (Fig. 1, com-

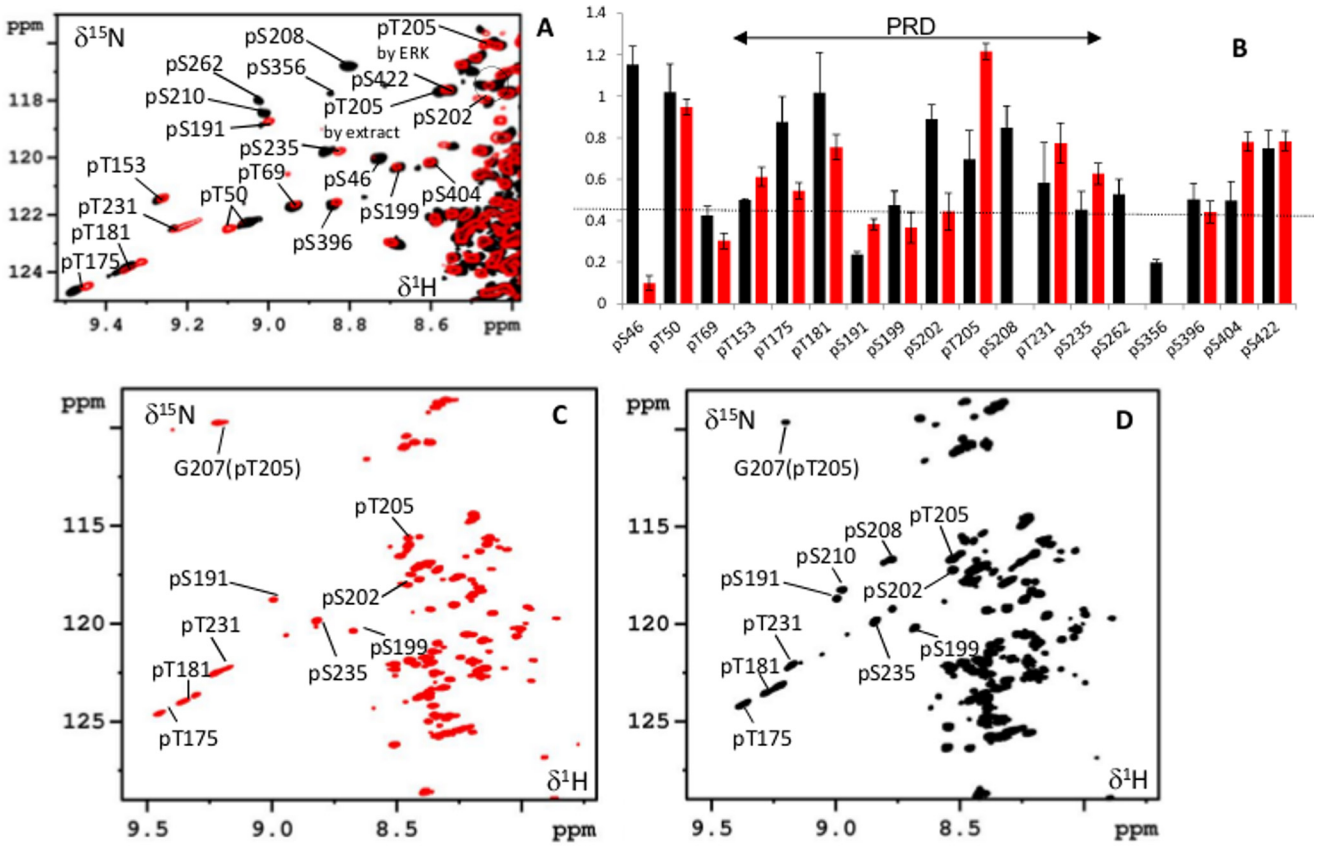

FIGURE 2. **Comparison of Tau phosphorylation by activated recombinant ERK2 and rat brain extracts.** *A*, overlaid details of $^{1}H,^{15}N$ HSQC two-dimensional spectra of phosphorylated Tau by activated ERK2 (in *red*) or by rat brain extract (in *black*). The enlarged region corresponds to the *boxed region* in Fig. 1. *C* and *D*, resonances corresponding to assigned phosphorylated Tau residues are annotated. *B*, level of phosphorylation for each Ser(P)-/Thr(P)-Tau residue presented as *black bars* for Tau phosphorylated by the rat brain extract and *red bars* by activated ERK2. Each experiment was repeated twice. S.D. around average value is shown by *error bars*. The level of phosphorylation is estimated based on the integrals of resonance peaks as described under "Experimental Procedures." *C* and *D*, $^{1}H,^{15}N$ HSQC two-dimensional spectrum of Tau-(165–245) modified by incubation at 37 °C for 3 h with activated recombinant ERK2 (*C*) or overnight with rat brain extract (*D*). The annotated resonances were assigned to phosphorylation sites by comparison with the $^{1}H,^{15}N$ HSQC two-dimensional spectrum of Tau protein phosphorylated by activated recombinant ERK2 or rat brain extract in the same conditions.

TABLE 1

Sequence specific assignment of resonances corresponding to phosphorylated residues in ERK phospho-Tau

^{1}H, ^{15}N, CA, and CB columns correspond to the chemical shifts (in ppm) of atoms from the assigned phospho-residues indicated in the first column. The amino acid type at the direct N terminus of each phospho-residue is displayed in column i-1 residue type and the chemical shifts of the corresponding CA and CB atoms in CA-1 and CB-1 columns.

Phosphorylated amino acids	^{15}N	^{1}H	CA	CB	CA-1	CB-1	i-1 residue type
	ppm	*ppm*	*ppm*	*ppm*	*ppm*	*ppm*	
Ser(P)-46	120.4	8.80	56.1	64.9	57.4	30.9	Glu
Thr(P)-50	123.5	9.30	61.1	72.2	55.6	30.2	Gln
Thr(P)-69	122.5	9.13	60.7	72.2	58.4	64.1	Ser
Thr(P)-153	121.8	9.35	61.1	72.2	52.4	19.4	Ala
Thr(P)-175	125.1	9.59	61.5	72.4	55.7	33.3	Lys
Thr(P)-181	124.5	9.49	61.3	72.4	55.9	33.3	Lys
Ser(P)-191	119.0	9.04	58.3	65.6	56.0	33.3	Lys
Ser(P)-199	120.6	8.71	56.0	65.0	57.7	64.3	Ser
Ser(P)-202	117.9	8.54	55.7	65.3	45.0	-	Gly
Thr(P)-205	117.1	8.62	60.4	71.8	45.0	-	Gly
Thr(P)-231	123.0	9.33	60.9	72.2	55.8	31.0	Arg
Ser(P)-235	120.0	8.85	55.8	65.2	56.5	33.3	Lys
Ser(P)-396	121.8	8.86	56.5	64.5	56.5	34.1	Lys
Ser(P)-404	120.4	8.66	55.9	70.0	61.7	70.0	Thr
Ser(P)-422	118.2	8.65	56.2	65.0	54.3	41.6	Asp

pare *panels D* and *B*). Comparison of two-dimensional spectra of Tau phosphorylated by either activated ERK2 or rat brain extracts showed that many resonances assigned to the ERK2 phosphorylated sites have a match in the brain extract phosphorylated Tau (Fig. 2, *A* and *B*). To confirm that the similarity in the phospho-Tau spectra reflects a shared phosphorylation pattern, phosphorylation sites were identified using three-dimensional triple resonance NMR spectroscopy on a $^{13}C,^{15}N$-labeled Tau phosphorylated *in vitro* by rat brain extract. The major modified sites of Tau correspond to Ser(P)-46, Thr(P)-50, Thr(P)-153, Thr(P)-175, Thr(P)-181, Ser(P)-202, Thr(P)-205, Ser(P)-208, Thr(P)-231, Ser(P)-262, Ser(P)-356, Ser(P)-396, Ser(P)-404, and Ser(P)-422 (Fig. 2). This analysis confirmed that the overlapping resonances in the two-dimensional spectra indeed correspond to the same phosphorylated residues. The level of phosphorylation for these residues is also similar between Tau phosphorylated by the rat brain extract or the activated ERK2 (Fig. 2*B*). A few additional Tau phosphorylation sites are also identified exclusively from the incubation with the rat brain extract including Ser(P)-208, Ser(P)-262, and Ser(P)-356 that are not proline-directed sites (Fig. 2*B*). Phosphorylation with the brain extract of Tau-(165–245) fragment, corresponding to the PRD, resulted in detection in the corresponding two-dimensional $^{1}H,^{15}N$ HSQC of resonances corresponding to phosphorylated residues. These phosphorylated sites matched those found in the PRD embedded in the full-length phosphorylated Tau protein (Fig. 2*D*), confirming the assignment. The data showed that the pattern of phosphoryla-

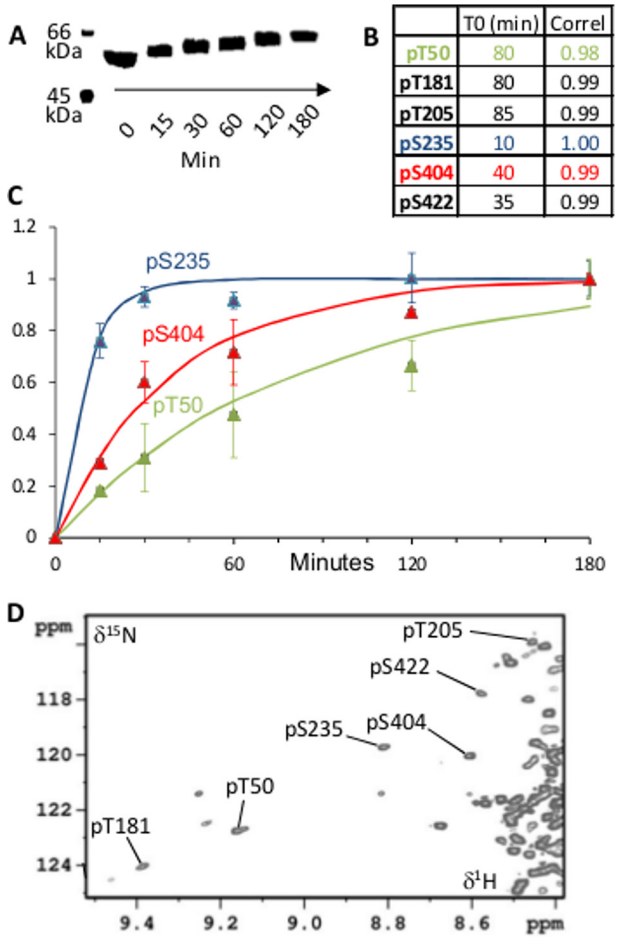

FIGURE 3. **Site-specific time course of *in vitro* Tau phosphorylation by activated ERK2.** *A*, 10% SDS-PAGE analysis of Tau incubated with activated ERK2 for increasing time periods. *B*, rate constant T0 in minutes and correlations. *C*, buildup of resonance integrals corresponding to Tau-phosphorylated residues, expressed as the fraction of maximum value reached during the 3-h reaction timeframe. Each data point is an average of three experiments from two independent samples. S.D. is indicated by *bars at each time point*. Data are fitted with a mono-exponential function 1-($e^{(-t/T0)}$) with time t and rate constant T0 in minutes (*B*). Correlation was calculated between the fit and the average experimental data. *D*, detail of ^{1}H,^{15}N HSQC two-dimensional spectrum of Tau incubated with activated ERK2 for 60 min. The enlarged region corresponds to the *boxed region* in Fig. 1, *C* and *D*. Resonances corresponding to assigned phosphorylated Tau residues are annotated.

tion obtained solely by ERK2 activity is similar to the one of the hyperphosphorylated Tau obtained by incubation with rat brain extract.

Aggregation Propensity of Tau Phosphorylated by Rat Brain Extracts or Activated ERK2—Tau phosphorylated by rat brain extract was shown to be able to self-assemble without the addition of an exogenous compound such as heparin (48). Given the similarity in the phosphorylation pattern of Tau phosphorylated by the rat brain extract or activated ERK2, we next evaluated the aggregation propensity of the later. Phosphorylated Tau samples by either rat brain extract or ERK2 were incubated at 35 °C, and the insoluble fraction of the sample was observed by electron microscopy. In both cases fibers of phospho-Tau were observed already after a 2-h incubation (Fig. 4). Filaments with diameters of 15–20 nm and lengths of several μm long were observed in both ERK2 or rat brain extract-phosphorylated Tau-aggregated samples. The fibers showed the typical helical appearance reported for PHF (49, 50). (Fig. 4, *A* and *C*). The aggregation is specific for the phosphorylated Tau samples as only rare isolated oligomers can be found in the control Tau sample incubated at 35 °C (Fig. 4*E*). However, the aggregated phosphoprotein only corresponded to a small fraction of the incubated samples and was, therefore, not positive for thioflavin detection, a fluorophore that detects amyloid fibril formation. We conclude that ERK2 by itself can generate a phosphorylated protein whose aggregation properties resemble those of the rat brain-phosphorylated protein. However, under our experimental conditions a robust aggregation of the rat brain extract-generated phospho-Tau was not observed.

Identification of the ERK2 Docking Site(s) on the Tau Protein—MAP kinases recognize their substrates not only by the phosphorylation (S/T)P motifs but also by docking motifs. We thus next investigated the mechanism of Tau recognition by ERK2. To map potential docking sites, two-dimensional spectra of [^{15}N]Tau mixed with recombinant ERK2 were compared with a reference spectrum from the [^{15}N]Tau protein free in solution (Fig. 5, *A* and *D*). The resonances in these spectra are sensitive to their chemical environment and the local protein dynamics, an interaction affecting their chemical shifts and/or intensities. At a 1:5 [^{15}N]Tau:ERK2 molar ratio, an interaction indeed translates into an important broadening for numerous resonances compared with the reference spectrum (Fig. 5, *A* and *D*). Assignment of the Tau protein resonances has been previously completed by us and others (51, 52) and was used to map the interaction region(s) based on the two-dimensional spectra perturbations. Peak intensities were compared for 187 resonances corresponding to residues dispersed along the 441-amino acid residue Tau sequence (Fig. 5*F*). The data showed interaction of ERK2 localized mainly in the MTBD of Tau (Tau-(244–372); also called K18; Ref. 1). To increase the resolution, the interaction experiment was repeated with Tau fragments, Tau-(165–245), corresponding to the PRD, and Tau-(244–372), corresponding to the MTBD (Figs. 5 and 6). The addition of ERK2 to [^{15}N]Tau-(165–245) resulted in minor perturbations of the resonances in the corresponding two-dimensional spectrum (Fig. 5*B*), whereas an interaction of ERK2 with Tau-(244–372) is clearly observed as the intensity of several resonances in its spectrum is affected (Figs. 5, *C* and *E*, and 6*A*). The intensity of the resonances corresponding to amino acids included in Tau-(274–288) and Tau-(306–318) segments strongly decreased in the presence of ERK2 (Fig. 6*A*, I/I0 <40%). These ERK2 docking sequences also correspond to, respectively, the PHF6* (^{275}VQIINK^{280}) and PHF6 (^{306}VQIVYK^{311}) peptides described as nuclei of Tau aggregation (53). Only the sequence of Tau-(274–288) can accommodate a canonical D-site ^{274}KVQIINKKLDL^{284} (Fig. 6*B*). Resonance intensities of residues in the Tau-(346–358) segment also showed a decrease upon ERK2 interaction but to a lesser extent (Fig. 6*A*, I/I0 below 60%). This region could correspond to a secondary binding site of interaction, although it is not clear if it fits a classical ERK2 docking site.

Because the PHF sequences, respectively, located in R2 and R3 repeated regions of the MTBD share similarities, it is likely that these peptides would have the same binding mode to ERK2. Yet only the PHF6* peptide can be matched to a D-site

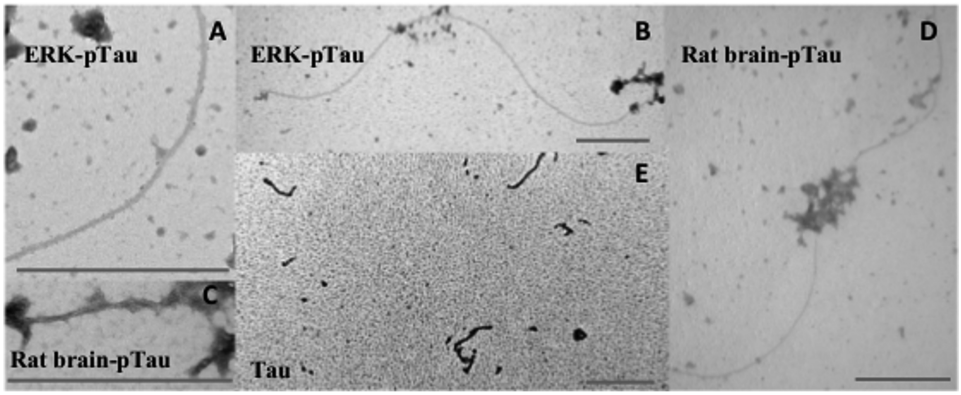

FIGURE 4. **Self-assembly of *in vitro* phosphorylated Tau.** Representative electron micrographs of the pellets of various Tau samples at 5 μM incubated at 35 °C for 2 h. *A* and *B*, phospho-Tau, modified by activated ERK2. *C* and *D*, phospho-Tau, modified by rat brain extract kinase activity. *E*, unphosphorylated Tau (incubated in phosphorylation mix without ATP), large field view. The *scale bars* in the *lower right corners* correspond to 500 nm.

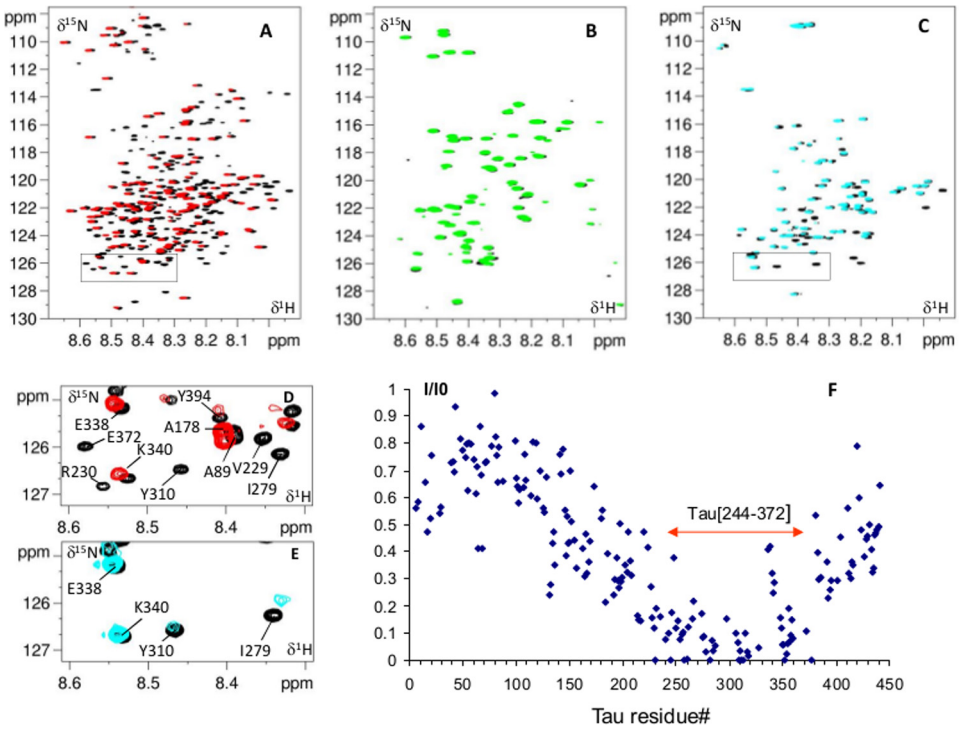

FIGURE 5. **ERK interacts with the MTBD of Tau.** *A–C*, overlaid two-dimensional spectra corresponding to free Tau (*black*) and Tau with a 5 molar excess of ERK (superimposed in *red*) (*A*), free Tau-(165–245) or PRD (*black*) and Tau-(165–245) with 1 mol eq of ERK2 (superimposed in *green*) (*B*), and free Tau-(244–372) or MTBD (*black*) and Tau-(244–372) with 1 molar excess of ERK2 (superimposed in *blue*) (*C*). *Boxed regions* in *A* and *C* are enlarged and annotated in *D* and *E*. *F*, relative intensities I/I0 of corresponding resonances in the two-dimensional spectra of Tau with 5 molar excess of ERK (*I*, *red* in *A*) or free in solution (I0, *black* in *A*) for residues along the Tau sequence.

sequence. To verify whether Tau interaction with ERK2 indeed involves a canonical D-site, a mutated ERK2 was used in our NMR binding assay. Replacement of two aspartic residues (D321N/D324N) in the D-site peptide binding pocket of ERK2 by asparagine residues disrupts the recognition of the positively charge residue ψ of the D-site docking peptide. The mutated D321N/D324N ERK2 has consequently a reduced affinity for the D-site peptides (28). However, we did not observe major differences in the NMR intensity profiles of [^{15}N]Tau-(244–372) in presence of ERK2 or D321N/D324N-mutated ERK2 (Fig. 6*A*), indicating no major impact of the mutations on the interaction.

Apparent K_D values were calculated to further characterize the Tau/ERK2 interaction using fluor NMR spectroscopy (54) to confirm that the main binding is located in the MTBD (Fig. 7). The Tau protein and Tau-(244–372) (MTBD) were labeled with fluor attached on the native Cys residues Cys-291 and Cys-322 along the sequence (Fig. 6*B*). Chemical shift value perturbation of the fluor signal along titration of the ERK2 protein on the labeled Tau or Tau fragment showed a saturation behavior typical of an interaction (Fig. 7). The similar apparent K_D values of 73 μM for Tau and 179 μM for Tau-(244–372) fragment indicated that the main binding indeed occurs within the Tau-(244–372) segment. The data demonstrate that the main binding sites of Tau for ERK2 are localized in the MTBD of Tau, in the Tau-(244–372) segment, outside of the regions containing ERK2 phosphorylation sites. The interaction is not mediated by a classical D-site interaction and shows a moderate

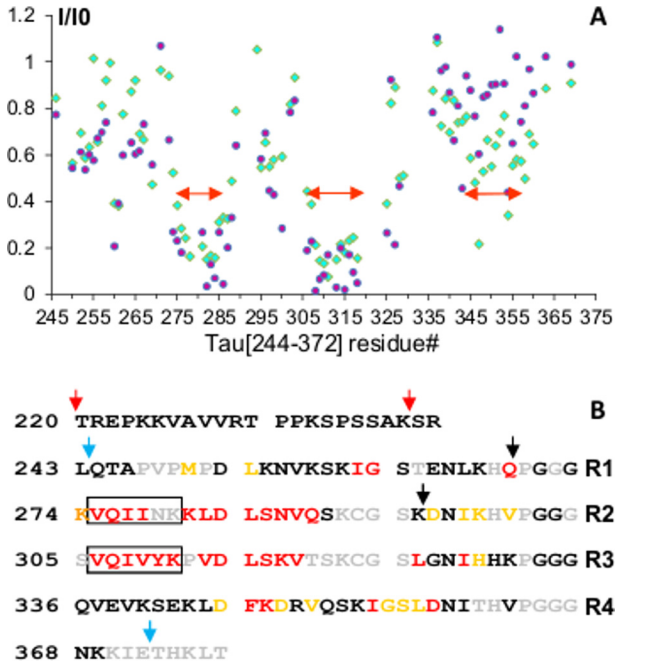

FIGURE 6. **ERK2 main interaction sites.** *A*, relative intensities I/I0 of corresponding resonances in the two-dimensional spectra of Tau-(244–372) with a 1 molar excess of ERK2 (I, *blue diamonds*) or D321N/D324N ERK2 (I, violet diamonds), *versus* free in solution (I0). *Double arrows* indicate the interaction regions along the sequence: Tau-(274–288), Tau-(306–318), and Tau-(346–358). *B*, sequence of Tau. Perturbations of resonance intensities are color-coded as *red* for residues with a I/I0 <0.5 and *orange* <0.6. Residues with no information for the corresponding resonance are in *gray*. Tau-(244–372) or MTBD is indicated by *blue arrows* along the sequence, and Tau-(220–240) and Tau-(271–294) peptides (Fig. 8) are indicated by *red* and *black arrows*, respectively. The PHF6* and PHF6 peptides in the R2 and R3 repeats, respectively, are *boxed*.

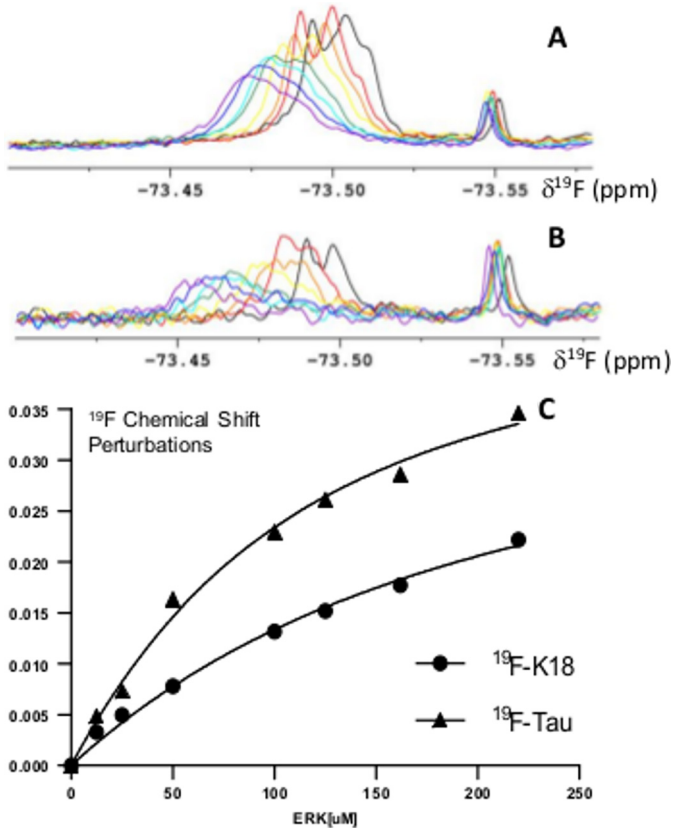

FIGURE 7. **Determination of K_D of Tau/ERK interaction.** Shown are superimposed one-dimensional Fluor NMR spectra of CF3-Tau-(244–372) (*A*) and CF3-Tau (*B*). *C*, saturation curves based on the chemical shift perturbation of the Fluor signal of CF3-Tau and CF3-Tau-(244–372). The signal of only one CF3-Cys was monitored along the titration, the second one being broadened.

affinity similar to the interaction of ERK2 by a minimal docking sequence reported for some of its protein partners (55).

Tau Peptides Interaction with ERK2 Kinase—Two peptides were next chosen to confirm whether they interact individually or not with the ERK2 docking site. The first peptide derived from the Tau sequence, Tau-(220–240) in the PRD, contains several ERK2 phosphorylation sites but no interaction site for ERK2. On the other hand, Tau-(271–294) contains the Tau-(274–284) sequence here above defined as an ERK2 docking site. As the Tau-(271–294) peptide showed a limited solubility (PHF6*), fusions with the SUMO protein were used both for the recombinant expression and two-dimensional spectra acquisition. SUMO being a small folded protein, the overlap with the Tau peptide signals was limited and, therefore, allowed a correct analysis of Tau resonances (Fig. 8). Overlay of the two-dimensional ^{1}H,^{15}N HSQC of the fusion peptides alone or mixed with ERK2 confirms that the resonance perturbations affected only those resonances corresponding to Tau peptides and not to SUMO fusion protein (Fig. 8). Resonances corresponding to Tau residues in SUMO-Tau-(220–240) are only slightly affected by the addition of ERK2 (Fig. 8, *A* and *C*). To the contrary, the addition of the kinase to the SUMO-Tau-(271–294) affected peak intensities of most of the resonances and principally residues 274 to 284 (Fig. 8, *B* and *D*). The peptides Tau-(220–240) and Tau-(271–294) behaved in their interaction with ERK2 in the same manner embedded in the protein or isolated from their context. The data confirmed the sequence

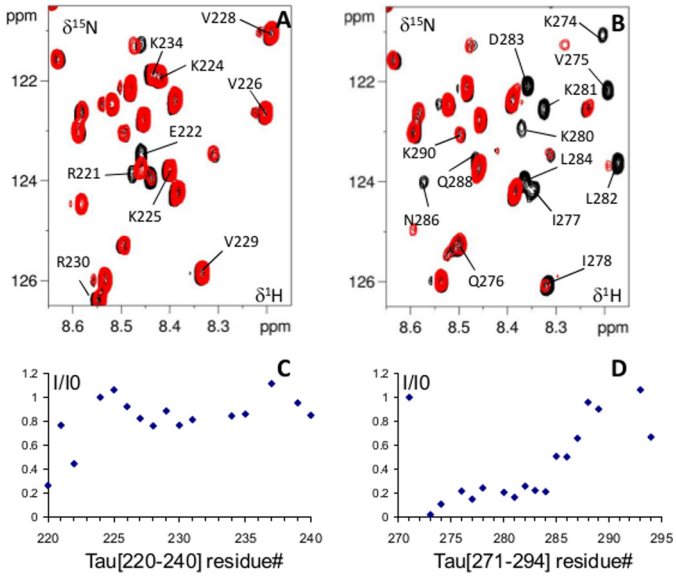

FIGURE 8. **Interaction of Tau peptides with ERK2.** *A* and *B*, detail of overlaid ^{1}H,^{15}N HSQC two-dimensional spectra of ^{15}N-His-SUMO Tau-(220–240) (*A*) and ^{15}N-His-SUMO Tau-(271–294) (*B*) free in solution (in *black*) or with 1 molar excess of ERK2 (superimposed in *red*). Relative intensities ratio I/I0 for corresponding resonances in these spectra are shown in *C* and *D*, respectively.

Lys-274 to Leu-284 as a docking site of ERK2. Despite the presence in the Tau-(220–240) of a predicted D docking site consensus sequence (Fig. 6*B*), no binding to ERK2 was observed.

Discussion

Using NMR spectroscopy, we identified Tau phosphorylation sites modified *in vitro* by the activated ERK2 and rat brain extracts. We demonstrate that Tau phosphorylation patterns observed with *in vitro* phosphorylation by ERK2 and rat brain extracts are similar, with most of the 17 (S/T)P motifs modified. Incorporation of 14–16 phosphates on (S/T)P sites per Tau molecule was reported by the MAPK activity purified from the brain extract (19). Our previous analysis of Tau phosphorylation patterns obtained *in vitro* by several other kinases showed that none has the capacity to modify such a large number of phosphorylation sites (43, 46, 47, 56). Phosphorylation by brain extracts is a method to obtain *in vitro* phosphorylated Tau (12, 38) with AD-like characteristics (48) such as a reduced electrophoretic mobility on SDS-PAGE and positive immunodetection of the AT8 epitope (12, 38) and the Ser(P)-396/Ser(P)-404 epitope (57). Our work shows that ERK2 by itself also has the potential to modify Tau into a phosphorylation state resembling Tau present in pathological AD state.

Early work by Iqbal and co-workers (48) showed that a Tau protein purified from AD brain or hyperphosphorylated *in vitro* by rat brain extract on 12–15 sites can form PHF-like aggregates. We observed fibers with a morphology typical of the helical pattern described for the PHF in both the activated ERK2 and rat brain extract-phosphorylated Tau samples incubated at 35 °C for 2 h. Tau phosphorylated solely by ERK2 on 15 phosphorylation sites, dispersed along the Tau sequence, behaved similarly as the rat brain extract-phosphorylated Tau in the aggregation assays. This aggregation propensity is specific to the phosphorylated Tau sample as we did not detect any PHF-like structures in the control Tau samples. However, the amount of fibers observed in our samples is small and could only be detected by electron microscopy performed on the pellet of our aggregation samples. Compared with the aggregation induced by the addition of heparin (58), the aggregation of the *in vitro* phosphorylated Tau affects only a small fraction of the sample. In agreement with this observation, a Tau protein phosphorylated on ~10 or ~20 phosphorylation sites in insect sf9 cells was recently reported to form oligomers and only a small fraction of fibrils (59). That the *in vitro* aggregation propensity under near physiological conditions of the *in vitro* phosphorylated Tau is low does not exclude that it could be a trigger in a cellular context, in which the aggregation process takes place on a long time scale (60). Nevertheless, there are only a few studies here above discussed that have explored the relationship between phosphorylation and aggregation. That phosphorylation is a causative event of Tau aggregation should be stated with more caution in regard of the data presented here by us and recently by others (59).

Our analytical characterization of Tau phosphorylation showed that ERK2 is promiscuous, as most of Tau (S/T)P motifs were phosphorylated. The question of how MAP kinases recognize specific substrates is only partially answered. We investigated the interaction of ERK2 with Tau and identified that it is mediated by two main docking sites. To our knowledge Tau is the first example of ERK2 protein substrate to contain a combination of docking sites. A similar combination of three D-docking sites was described in the regulatory disordered N-terminal region of MKK7 (MAP kinase kinase 7) used for the specific recognition by the JNK MAP kinase (61, 62). Another type of a modular system of recognition was previously proposed consisting of a combination of the D-docking site and F-docking site, although in this case it corresponds to two distinct binding grooves of ERK2 (34). Two binding sites on the substrates for one recognition groove of ERK2 allows the formation of a dynamic complex (63), defined as involving more than two transient interfaces between the binding partners. The presence of a high number of interaction sites on a flexible ligand such as Tau, termed allovalency, increases the probability of the rebinding of the protein partner (64, 65).

Comparison of the Tau interacting peptides with the degenerate ERK2 recognition sequence $\Psi_{1-3}X_{3-7}\phi X\phi$ (with Ψ for Arg/Lys residues, X for any residue, and ϕ for hydrophobic residues, the indices corresponding to the number of residues (29, 30) shows that only the first peptide Tau-(274–284) corresponds to predicted classical D-docking (Fig. 6*B*). We additionally showed that a mutated ERK2 with two Asp residues replaced by Asn residues in its docking pocket (D321N/D324N) to compromise interaction with the Ψ residue in the D-peptide (28) still binds Tau-(244–372) in the same manner as the wild type ERK2 (Fig. 6*A*). Some docking interactions of ERK2 have been reported to be limited to the hydrophobic pocket in the D-peptide binding site (31).This is the case of the PEA-15 protein, as seen in the crystal structure of PEA15-ERK2 complex. The structure also reveals a C-to-N reverse binding compared with the classical D-peptide interaction. This type of docking interaction is also characterized by a weaker affinity, with a dissociation constant of 18 μM reported for the PEA15/ERK2 interaction (31). This value is closer to the 10 μM range that we here found for the Tau/ERK2 interaction than the submicromolar range values reported for the canonical docking interaction of ERK2 with D-site peptides (30, 55). It was proposed that the minimal interaction mediated by the hydrophobic pocket of ERK2 is a hallmark of moderate affinity regulatory interactions (31). We showed that the Tau-(165–245) fragment does not contain a docking site for ERK2. Nevertheless, phosphorylation of Tau-(165–245) by activated ERK2 showed a similar pattern and level of phosphorylation as with the full-length Tau substrate (Fig. 2). This suggests that the enzymatic activity is not affected by the docking and that the phosphorylation of the PRD might not require the ERK2 docking in the MTBD, at least in the equilibrium conditions of our experiments. The essentiality of docking sites for ERK2 to exert its efficient kinase activity is not established (29, 66, 67). Kinetic studies demonstrate that docking sites that interact with either the D-recruitment site or the F-recruitment site have little effect on the intrinsic catalytic activity of ERK2 (66). In a proteomic study, a D-docking peptide was found only on 17% of the substrates within 20 amino acids of the phospho site (67). However, a peptide-based study shows to the contrary, that a docking site is necessary to mimic a ERK2 substrate (29). It might be in the case of Tau that the docking sites are crucial to manage formation of regulatory complexes in a cellular context rather than to stimulate activity toward the protein partners (31).

Activation of ERK1/2 is increased in AD neurons (68), is found in association with abnormally phosphorylated early Tau deposits (69), and is linked to the progression of the neurofibrillary degeneration through the Braak stages of AD (35, 60). Activation of ERK1/2 also responds to fibrillar amyloid β deposits in mature hippocampal neuronal culture (70) and to increased activity of inositol-trisphosphate 3-kinase B (37) and oxidative stress (71), all affecting Tau phosphorylation. ERK1/2 phosphorylation of Tau could thus take place in cells upon stress signaling or once the phosphorylation fails to be counteracted by an efficient dephosphorylation. ERK is thus accordingly considered as a Tau kinase that could be involved in AD pathophysiology. We have reinforced this view by showing that ERK2 has the capacity by itself to phosphorylate Tau on many sites. These results support the hypothesis that ERK activation under stress conditions might have a detrimental effect for Tau function and participate in AD physiopathology.

Author Contributions—H. Q., S. P., and I. L. conducted most of the experiments, F.-X. C. conducted most NMR data acquisition, H. Q. and I. L. performed NMR data analysis, B. C. prepared the rat brain extract and advised on the manuscript, I. L., S. P., G. L., J. G., and H. Q. wrote the manuscript, and I. L., S. P., G. L., and J. G. conceived the idea for the project. All authors reviewed the results and approved the final version of the manuscript.

Acknowledgments—We thank O. Dounane (UMR1195) for technical assistance and L. Brunet (Bio Imaging Center of Lille, Lille1 campus) for access to instruments and technical advices. The NMR facilities were supported by the Région Nord, CNRS, Pasteur Institute of Lille, European Community (FEDER), French Research Ministry and Lille University.

References

1. Gustke, N., Trinczek, B., Biernat, J., Mandelkow, E. M., and Mandelkow, E. (1994) Domains of tau protein and interactions with microtubules. *Biochemistry* **33,** 9511–9522
2. Goode, B. L., Denis, P. E., Panda, D., Radeke, M. J., Miller, H. P., Wilson, L., and Feinstein, S. C. (1997) Functional interactions between the proline-rich and repeat regions of tau enhance microtubule binding and assembly. *Mol. Biol. Cell.* **8,** 353–365
3. Alonso, A. C., Zaidi, T., Grundke-Iqbal, I., and Iqbal, K. (1994) Role of abnormally phosphorylated tau in the breakdown of microtubules in Alzheimer disease. *Proc. Natl. Acad. Sci. U.S.A.* **91,** 5562–5566
4. Stoothoff, W. H., and Johnson, G. V. (2005) Tau phosphorylation: physiological and pathological consequences. *Biochim. Biophys. Acta* **1739,** 280–297
5. Götz, J., Gladbach, A., Pennanen, L., van Eersel, J., Schild, A., David, D., and Ittner, L. M. (2010) Animal models reveal role for tau phosphorylation in human disease. *Biochim. Biophys. Acta* **1802,** 860–871
6. Grundke-Iqbal, I., Iqbal, K., Tung, Y. C., Quinlan, M., Wisniewski, H. M., and Binder, L. I. (1986) Abnormal phosphorylation of the microtubule-associated protein tau (tau) in Alzheimer cytoskeletal pathology. *Proc. Natl. Acad. Sci. U.S.A.* **83,** 4913–4917
7. Martin, L., Latypova, X., Wilson, C. M., Magnaudeix, A., Perrin, M. L., Yardin, C., and Terro, F. (2013) Tau protein kinases: involvement in Alzheimer's disease. *Ageing Res. Rev.* **12,** 289–309
8. Hasegawa, M., Morishima-Kawashima, M., Takio, K., Suzuki, M., Titani, K., and Ihara, Y. (1992) Protein sequence and mass spectrometric analyses of tau in the Alzheimer's disease brain. *J. Biol. Chem.* **267,** 17047–17054
9. Morishima-Kawashima, M., Hasegawa, M., Takio, K., Suzuki, M., Yoshida, H., Watanabe, A., Titani, K., and Ihara, Y. (1995) Hyperphosphorylation of tau in PHF. *Neurobiol. Aging* **16,** 365–371; discussion 371–380
10. Morris, M., Knudsen, G. M., Maeda, S., Trinidad, J. C., Ioanoviciu, A., Burlingame, A. L., and Mucke, L. (2015) Tau post-translational modifications in wild-type and human amyloid precursor protein transgenic mice. *Nat. Neurosci.* **18,** 1183–1189
11. Funk, K. E., Thomas, S. N., Schafer, K. N., Cooper, G. L., Liao, Z., Clark, D. J., Yang, A. J., and Kuret, J. (2014) Lysine methylation is an endogenous post-translational modification of tau protein in human brain and a modulator of aggregation propensity. *Biochem. J.* **462,** 77–88
12. Biernat, J., Mandelkow, E. M., Schröter, C., Lichtenberg-Kraag, B., Steiner, B., Berling, B., Meyer, H., Mercken, M., Vandermeeren, A., and Goedert, M. (1992) The switch of tau protein to an Alzheimer-like state includes the phosphorylation of two serine-proline motifs upstream of the microtubule binding region. *EMBO J.* **11,** 1593–1597
13. Jeganathan, S., Hascher, A., Chinnathambi, S., Biernat, J., Mandelkow, E. M., and Mandelkow, E. (2008) Proline-directed pseudo-phosphorylation at AT8 and PHF1 epitopes induces a compaction of the paperclip folding of Tau and generates a pathological (MC-1) conformation. *J. Biol. Chem.* **283,** 32066–32076
14. Baumann, K., Mandelkow, E. M., Biernat, J., Piwnica-Worms, H., and Mandelkow, E. (1993) Abnormal Alzheimer-like phosphorylation of tau protein by cyclin-dependent kinases cdk2 and cdk5. *FEBS Lett.* **336,** 417–424
15. Kobayashi, S., Ishiguro, K., Omori, A., Takamatsu, M., Arioka, M., Imahori, K., and Uchida, T. (1993) A cdc2-related kinase PSSALRE/cdk5 is homologous with the 30-kDa subunit of tau protein kinase II, a proline-directed protein kinase associated with microtubule. *FEBS Lett.* **335,** 171–175
16. Ishiguro, K., Shiratsuchi, A., Sato, S., Omori, A., Arioka, M., Kobayashi, S., Uchida, T., and Imahori, K. (1993) Glycogen synthase kinase 3β is identical to tau protein kinase I generating several epitopes of paired helical filaments. *FEBS Lett.* **325,** 167–172
17. Reynolds, C. H., Utton, M. A., Gibb, G. M., Yates, A., and Anderton, B. H. (1997) Stress-activated protein kinase/c-jun N-terminal kinase phosphorylates tau protein. *J Neurochem.* **68,** 1736–1744
18. Reynolds, C. H., Nebreda, A. R., Gibb, G. M., Utton, M. A., and Anderton, B. H. (1997) Reactivating kinase/p38 phosphorylates tau protein *in vitro*. *J. Neurochem.* **69,** 191–198
19. Drewes, G., Lichtenberg-Kraag, B., Döring, F., Mandelkow, E. M., Biernat, J., Goris, J., Dorée, M., and Mandelkow, E. (1992) Mitogen activated protein (MAP) kinase transforms tau protein into an Alzheimer-like state. *EMBO J.* **11,** 2131–2138
20. Mazanetz, M. P., and Fischer, P. M. (2007) Untangling tau hyperphosphorylation in drug design for neurodegenerative diseases. *Nat. Rev. Drug. Discov.* **6,** 464–479
21. Anderson, N. G., Maller, J. L., Tonks, N. K., and Sturgill, T. W. (1990) Requirement for integration of signals from two distinct phosphorylation pathways for activation of MAP kinase. *Nature* **343,** 651–653
22. Boulton, T. G., Yancopoulos, G. D., Gregory, J. S., Slaughter, C., Moomaw, C., Hsu, J., and Cobb, M. H. (1990) An insulin-stimulated protein kinase similar to yeast kinases involved in cell cycle control. *Science* **249,** 64–67
23. Seger, R., Ahn, N. G., Boulton, T. G., Yancopoulos, G. D., Panayotatos, N., Radziejewska, E., Ericsson, L., Bratlien, R. L., Cobb, M. H., and Krebs, E. G. (1991) Microtubule-associated protein 2 kinases, ERK1 and ERK2, undergo autophosphorylation on both tyrosine and threonine residues: implications for their mechanism of activation. *Proc. Natl. Acad. Sci. U.S.A.* **88,** 6142–6146
24. Zhang, F., Strand, A., Robbins, D., Cobb, M. H., and Goldsmith, E. J. (1994) Atomic structure of the MAP kinase ERK2 at 2.3 Å resolution. *Nature* **367,** 704–711
25. Canagarajah, B. J., Khokhlatchev, A., Cobb, M. H., and Goldsmith, E. J. (1997) Activation mechanism of the MAP kinase ERK2 by dual phosphorylation. *Cell* **90,** 859–869
26. Adams, P. D., Sellers, W. R., Sharma, S. K., Wu, A. D., Nalin, C. M., and Kaelin, W. G., Jr. (1996) Identification of a cyclin-cdk2 recognition motif present in substrates and p21-like cyclin-dependent kinase inhibitors. *Mol. Cell Biol.* **16,** 6623–6633
27. Brown, N. R., Noble, M. E., Endicott, J. A., and Johnson, L. N. (1999) The

structural basis for specificity of substrate and recruitment peptides for cyclin-dependent kinases. *Nat. Cell Biol.* **1,** 438–443
28. Tanoue, T., Adachi, M., Moriguchi, T., and Nishida, E. (2000) A conserved docking motif in MAP kinases common to substrates, activators and regulators. *Nat. Cell Biol.* **2,** 110–116
29. Fernandes, N., Bailey, D. E., Vanvranken, D. L., and Allbritton, N. L. (2007) Use of docking peptides to design modular substrates with high efficiency for mitogen-activated protein kinase extracellular signal-regulated kinase. *ACS Chem. Biol.* **2,** 665–673
30. Garai, Á., Zeke, A., Gógl, G., Törő, I., Fördős, F., Blankenburg, H., Bárkai, T., Varga, J., Alexa, A., Emig, D., Albrecht, M., and Reményi, A. (2012) Specificity of linear motifs that bind to a common mitogen-activated protein kinase docking groove. *Sci. Signal.* **5,** ra74
31. Liu, S., Sun, J. P., Zhou, B., and Zhang, Z. Y. (2006) Structural basis of docking interactions between ERK2 and MAP kinase phosphatase 3. *Proc. Natl. Acad. Sci. U.S.A.* **103,** 5326–5331
32. Zhou, T., Sun, L., Humphreys, J., and Goldsmith, E. J. (2006) Docking interactions induce exposure of activation loop in the MAP kinase ERK2. *Structure* **14,** 1011–1019
33. Ma, W., Shang, Y., Wei, Z., Wen, W., Wang, W., and Zhang, M. (2010) Phosphorylation of DCC by ERK2 is facilitated by direct docking of the receptor P1 domain to the kinase. *Structure* **18,** 1502–1511
34. Jacobs, D., Glossip, D., Xing, H., Muslin, A. J., and Kornfeld, K. (1999) Multiple docking sites on substrate proteins form a modular system that mediates recognition by ERK MAP kinase. *Genes Dev.* **13,** 163–175
35. Pei, J. J., Braak, H., An, W. L., Winblad, B., Cowburn, R. F., Iqbal, K., and Grundke-Iqbal, I. (2002) Up-regulation of mitogen-activated protein kinases ERK1/2 and MEK1/2 is associated with the progression of neurofibrillary degeneration in Alzheimer's disease. *Brain Res. Mol. Brain Res.* **109,** 45–55
36. Swatton, J. E., Sellers, L. A., Faull, R. L., Holland, A., Iritani, S., and Bahn, S. (2004) Increased MAP kinase activity in Alzheimer's and Down syndrome but not in schizophrenia human brain. *Eur. J. Neurosci.* **19,** 2711–2719
37. Stygelbout, V., Leroy, K., Pouillon, V., Ando, K., D'Amico, E., Jia, Y., Luo, H. R., Duyckaerts, C., Erneux, C., Schurmans, S., and Brion, J. P. (2014) Inositol trisphosphate 3-kinase B is increased in human Alzheimer brain and exacerbates mouse Alzheimer pathology. *Brain* **137,** 537–552
38. Goedert, M., Jakes, R., Crowther, R. A., Six, J., Lübke, U., Vandermeeren, M., Cras, P., Trojanowski, J. Q., and Lee, V. M. (1993) The abnormal phosphorylation of tau protein at Ser-202 in Alzheimer disease recapitulates phosphorylation during development. *Proc. Natl. Acad. Sci. U.S.A.* **90,** 5066–5070
39. Luna-Vargas, M. P., Christodoulou, E., Alfieri, A., van Dijk, W. J., Stadnik, M., Hibbert, R. G., Sahtoe, D. D., Clerici, M., Marco, V. D., Littler, D., Celie, P. H., Sixma, T. K., and Perrakis, A. (2011) Enabling high-throughput ligation-independent cloning and protein expression for the family of ubiquitin specific proteases. *J. Struct. Biol.* **175,** 113–119
40. Prabakaran, S., Everley, R. A., Landrieu, I., Wieruszeski, J. M., Lippens, G., Steen, H., and Gunawardena, J. (2011) Comparative analysis of Erk phosphorylation suggests a mixed strategy for measuring phospho-form distributions. *Mol. Syst. Biol.* **7,** 482
41. Weisemann, R., Rüterjans, H., and Bermel, W. (1993) Three-dimensional triple-resonance NMR techniques for the sequential assignment of NH and ^{15}N resonances in ^{15}N- and ^{13}C-labelled proteins. *J. Biomol. NMR* **3,** 113–120
42. Bienkiewicz, E. A., and Lumb, K. J. (1999) Random-coil chemical shifts of phosphorylated amino acids. *J. Biomol. NMR* **15,** 203–206
43. Landrieu, I., Lacosse, L., Leroy, A., Wieruszeski, J. M., Trivelli, X., Sillen, A., Sibille, N., Schwalbe, H., Saxena, K., Langer, T., and Lippens, G. (2006) NMR analysis of a Tau phosphorylation pattern. *J. Am. Chem. Soc.* **128,** 3575–3583
44. Theillet, F.-X., Smet-Nocca, C., Liokatis, S., Thongwichian, R., Kosten, J., Yoon, M.-K., Kriwacki, R. W., Landrieu, I., Lippens, G., and Selenko, P. (2012) Cell signaling, post-translational protein modifications and NMR spectroscopy. *J. Biomol. NMR* **54,** 217–236
45. Theillet, F. X., Rose, H. M., Liokatis, S., Binolfi, A., Thongwichian, R., Stuiver, M., and Selenko, P. (2013) Site-specific NMR mapping and time-resolved monitoring of serine and threonine phosphorylation in reconstituted kinase reactions and mammalian cell extracts. *Nat. Protoc.* **8,** 1416–1432
46. Amniai, L., Barbier, P., Sillen, A., Wieruszeski, J. M., Peyrot, V., Lippens, G., and Landrieu, I. (2009) Alzheimer disease-specific phosphoepitopes of Tau interfere with assembly of tubulin but not binding to microtubules. *FASEB J.* **23,** 1146–1152
47. Leroy, A., Landrieu, I., Huvent, I., Legrand, D., Codeville, B., Wieruszeski, J. M., and Lippens, G. (2010) Spectroscopic studies of GSK3β phosphorylation of the neuronal tau protein and its interaction with the N-terminal domain of apolipoprotein E. *J. Biol. Chem.* **285,** 33435–33444
48. Alonso, A., Zaidi, T., Novak, M., Grundke-Iqbal, I., and Iqbal, K. (2001) Hyperphosphorylation induces self-assembly of tau into tangles of paired helical filaments/straight filaments. *Proc. Natl. Acad. Sci. U.S.A.* **98,** 6923–6928
49. Kidd, M. (1963) Paired helical filaments in electron microscopy of Alzheimer's disease. *Nature* **197,** 192–193
50. Wischik, C. M., Crowther, R. A., Stewart, M., and Roth, M. (1985) Subunit structure of paired helical filaments in Alzheimer's disease. *J. Cell Biol.* **100,** 1905–1912
51. Smet, C., Leroy, A., Sillen, A., Wieruszeski, J. M., Landrieu, I., and Lippens, G. (2004) Accepting its random coil nature allows a partial NMR assignment of the neuronal Tau protein. *Chembiochem* **5,** 1639–1646
52. Mukrasch, M. D., Bibow, S., Korukottu, J., Jeganathan, S., Biernat, J., Griesinger, C., Mandelkow, E., and Zweckstetter, M. (2009) Structural polymorphism of 441-residue tau at single residue resolution. *PLos Biol.* **7,** e34
53. von Bergen, M., Friedhoff, P., Biernat, J., Heberle, J., Mandelkow, E. M., and Mandelkow, E. (2000) Assembly of tau protein into Alzheimer paired helical filaments depends on a local sequence motif (^{306}VQIVYK^{311}) forming β structure. *Proc. Natl. Acad. Sci. U.S.A.* **97,** 5129–5134
54. Marsh, E. N., and Suzuki, Y. (2014) Using ^{19}F NMR to probe biological interactions of proteins and peptides. *ACS Chem. Biol.* **9,** 1242–1250
55. Mace, P. D., Wallez, Y., Egger, M. F., Dobaczewska, M. K., Robinson, H., Pasquale, E. B., and Riedl, S. J. (2013) Structure of ERK2 bound to PEA-15 reveals a mechanism for rapid release of activated MAPK. *Nat. Commun.* **4,** 1681
56. Lippens, G., Amniai, L., Wieruszeski, J. M., Sillen, A., Leroy, A., and Landrieu, I. (2012) Towards understanding the phosphorylation code of tau. *Biochem. Soc. Trans.* **40,** 698–703
57. Lichtenberg-Kraag, B., Mandelkow, E. M., Biernat, J., Steiner, B., Schröter, C., Gustke, N., Meyer, H. E., and Mandelkow, E. (1992) Phosphorylation-dependent epitopes of neurofilament antibodies on tau protein and relationship with Alzheimer tau. *Proc. Natl. Acad. Sci. U.S.A.* **89,** 5384–5388
58. Goedert, M., Jakes, R., Spillantini, M. G., Hasegawa, M., Smith, M. J., and Crowther, R. A. (1996) Assembly of microtubule-associated protein tau into Alzheimer-like filaments induced by sulphated glycosaminoglycans. *Nature* **383,** 550–553
59. Tepper, K., Biernat, J., Kumar, S., Wegmann, S., Timm, T., Hübschmann, S., Redecke, L., Mandelkow, E. M., Müller, D. J., and Mandelkow, E. (2014) Oligomer formation of tau protein hyperphosphorylated in cells. *J. Biol. Chem.* **289,** 34389–34407
60. Braak, H., and Braak, E. (1991) Neuropathological staging of Alzheimer-related changes. *Acta Neuropathol.* **82,** 239–259
61. Ho, D. T., Bardwell, A. J., Grewal, S., Iverson, C., and Bardwell, L. (2006) Interacting JNK-docking sites in MKK7 promote binding and activation of JNK mitogen-activated protein kinases. *J. Biol. Chem.* **281,** 13169–13179
62. Kragelj, J., Palencia, A., Nanao, M. H., Maurin, D., Bouvignies, G., Blackledge, M., and Jensen, M. R. (2015) Structure and dynamics of the MKK7-JNK signaling complex. *Proc. Natl. Acad. Sci. U.S.A.* **112,** 3409–3414
63. Mittag, T., Marsh, J., Grishaev, A., Orlicky, S., Lin, H., Sicheri, F., Tyers, M., and Forman-Kay, J. D. (2010) Structure/function implications in a dynamic complex of the intrinsically disordered Sic1 with the Cdc4 subunit of an SCF ubiquitin ligase. *Structure* **18,** 494–506
64. Klein, P., Pawson, T., and Tyers, M. (2003) Mathematical modeling suggests cooperative interactions between a disordered polyvalent ligand and a single receptor site. *Curr. Biol.* **13,** 1669–1678
65. Ubersax, J. A., and Ferrell, J. E., Jr. (2007) Mechanisms of specificity in protein phosphorylation. *Nat. Rev. Mol. Cell Biol.* **8,** 530–541

66. Lee, S., Warthaka, M., Yan, C., Kaoud, T. S., Ren, P., and Dalby, K. N. (2011) Examining docking interactions on ERK2 with modular peptide substrates. *Biochemistry* **50,** 9500–9510
67. Courcelles, M., Frémin, C., Voisin, L., Lemieux, S., Meloche, S., and Thibault, P. (2013) Phosphoproteome dynamics reveal novel ERK1/2 MAP kinase substrates with broad spectrum of functions. *Mol. Syst. Biol.* **9,** 669
68. Arendt, T., Holzer, M., Grossmann, A., Zedlick, D., and Brückner, M. K. (1995) Increased expression and subcellular translocation of the mitogen-activated protein kinase kinase and mitogen-activated protein kinase in Alzheimer's disease. *Neuroscience* **68,** 5–18
69. Ferrer, I., Blanco, R., Carmona, M., Ribera, R., Goutan, E., Puig, B., Rey, M. J., Cardozo, A., Viñals, F., and Ribalta, T. (2001) Phosphorylated map kinase (ERK1, ERK2) expression is associated with early tau deposition in neurones and glial cells, but not with increased nuclear DNA vulnerability and cell death, in Alzheimer disease, Pick's disease, progressive supranuclear palsy, and corticobasal degeneration. *Brain Pathol.* **11,** 144–158
70. Ferreira, A., Lu, Q., Orecchio, L., and Kosik, K. S. (1997) Selective phosphorylation of adult tau isoforms in mature hippocampal neurons exposed to fibrillar Aβ. *Mol. Cell Neurosci.* **9,** 220–234
71. Perry, G., Roder, H., Nunomura, A., Takeda, A., Friedlich, A. L., Zhu, X., Raina, A. K., Holbrook, N., Siedlak, S. L., Harris, P. L., and Smith, M. A. (1999) Activation of neuronal extracellular receptor kinase (ERK) in Alzheimer disease links oxidative stress to abnormal phosphorylation. *Neuroreport* **10,** 2411–2415

Characterization of Neuronal Tau Protein as a Target of Extracellular Signal-regulated Kinase

Haoling Qi, Sudhakaran Prabakaran, François-Xavier Cantrelle, Béatrice Chambraud, Jeremy Gunawardena, Guy Lippens and Isabelle Landrieu

J. Biol. Chem. 2016, 291:7742-7753.
doi: 10.1074/jbc.M115.700914 originally published online February 8, 2016